Hollow states of lithium

Micheal J. Conneely
Department of Mathematical Physics, National University of Ireland, Galway, Galway, Ireland

Lester Lipsky
Department of Computer Science and Engineering, University of Connecticut, Storrs, Connecticut 06269-3155
(Received 12 August 1999; published 17 February 2000)

The energies, effective quantum numbers, classifications, and configuration mixings of the triply excited states of lithium in the energy range of 140–160 eV above the ground state are described in detail based on calculations using the truncated diagonalization method. A total of 30 Rydberg series with symmetries $^2S^o$, $^2S^e$, $^2P^o$, $^2P^e$, and $^2D^e$ are investigated. The perturbation of a Rydberg series by an isolated state, or by another series, is examined and discussed. Differences in the literature on the designation of certain states are pointed out, and our results are compared with recent theoretical and experimental data. We observe that the configuration interactions previously described for two-electron systems [i.e., the mixing of the $(2s)^2$ and $(2p)^2\,^1S^e$ states] remain when a third electron is added.

PACS number(s): 31.15.−p, 31.50.+w, 32.30.−r, 32.80.Dz

I. INTRODUCTION

The hollow states of lithium have recently been the subject of intense experimental and theoretical interest [1–14]. These are the triply excited states of lithium (or lithiumlike ions) where both $1s$-shell orbitals are vacant. The doubly excited states of helium, where the K shell is empty, are also examples of hollow atomic states. These were first studied experimentally more than 30 years ago and first described theoretically by Fano [15]. The study of these doubly excited states of helium and heliumlike ions in the past three decades has resulted in new classification schemes for such states. Some of the schemes have been based on group theoretic considerations [16] and other more heuristic ones, based on configuration mixings [17] and [22].

Lithium, with one additional electron outside the $(1s)^2$ core, is the simplist open-shell many-electron system. Simultaneous excitation of all three electrons can create hollow atoms of the type n_1l_1,n_2l_2,n_3l_3 with n_1, n_2, and n_3 all greater than or equal to 2. In such situations, with the simultaneous excitation of the electrons to large distances from the nucleus, correlation effects become important, since the dominant role of the nuclear Coulomb potential is reduced. Electron correlations are described within the independent-particle model by the superposition of configurations of the same L, S, π symmetry. In this paper, for each L, S π symmetry, we shall consider states where all of n_1, n_2, or n_3 are greater than or equal to 2, and use configuration mixings to classify these states, analogous to the method used for helium and heliumlike ions [17].

The first reported observations of triply excited $2l_12l_22l_3$ states in lithium were in collision experiments [18,19]. The first photoexcitation experiment on hollow lithium was carried out recently [1] and provided data on the lowest $(2s)^22p^2P^o$ resonance (at ≈142 eV above the ground state of lithium). Subsequent experiments involving the use of photoion and photoelectron spectrometries determined the energies and widths of higher-lying resonances. Several Rydberg series have been measured and identified. Theoretical calculations using the R-matrix approximation and the saddle-point technique have been used to identify these resonances. The truncated diagonalization method (TDM) has also been used to calculate the energies and wave functions of these triply excited states [20] and also of doubly excited states where there is just one vacancy in the K shell [21]. One of the advantages of this method is that it yields complete Rydberg series converging on the doubly excited states of Li^+ all at once. The various series and levels are almost always identifiable by their configuration mixings and quantum defects.

In this paper we use the TDM method to calculate the energies of the triply excited states of lithium for various L, S, π symmetries and compare our results with those of other calculations and with experiment where available. In the close-coupling procedure used in the calculations of Berrington and Nagazaki [23] (hereafter referred to as BN) and Vo Ky *et al.*, [24] the wave function is expanded in a linear combination of products of target states ϕ_i with some unknown function for the additional electron, $F_\mu(r)$. The unknown functions $F_\mu(r)$ satisfy second-order integro-differential equations obtained from the Kohn variational principle, which are then solved using the R-matrix method. The positions and widths of the resonances are obtained by phase-shift analysis in the case of BN, or in the case of Vo Ky *et al.*, from the Fano profile of the photoionization cross sections. As has been discussed by BN, the accuracy of these close-coupling calculations will depend on the selection and the number of target states included in the expansion. In these calculations, the energy shift, Δ_n, that comes from interactions of the closed channels with the open channels is automatically accounted for.

The interaction of the closed and open channels is also accounted for in Chung's calculations [13,14,27] where the saddle-point method is combined with the complex rotation method to yield the energies and widths of the resonances. In this method, the wave function is written as $\Psi=\Psi_c+\Psi_o$, where Ψ_c and Ψ_o are the closed and open channels, respectively. Ψ_c contains linear and nonlinear parameters and is

determined, first, by the saddle-point method, i.e., by an energy optimization process. The open channel component is written as a linear combination of the target states and the wave function of the outgoing electron. In the calculations, the nonlinear parameters obtained from the saddle-point calculations for Ψ_c are retained, but the linear parameters are recalculated to allow for the full interaction between the closed channel and open channel wave functions.

In the TDM method, the wave functions are expanded in terms of a given set (albeit finite) of basis functions, and the expansion coefficients are chosen so that the energies are minimized, which is equivalent to diagonalizing the Hamiltonian matrix. The lowest eigenvalues, E_n, of this truncated matrix are the energies quoted here. The E_n's are not measurable experimentally. What is measured is $\mathcal{E}_n = E_n + \Delta_n$, where Δ_n is the shift in energy due to the interaction with the open channels. This energy shift has been calculated by Chung and is in general small, of the order of a few meV, but in certain cases can be of the order of 0.1 eV.

In general there is excellent agreement among the different methods in the classification and identification of the triply excited states of the lithium atom in the energy range of 140–160 eV above the ground state. In particular, we find a one-to-one correspondence between our results and those of BN, the only exception being the lowest state of $(2p)^2\,{}^1D^e ns\,{}^2D^e$ series.

In Sec. II we give a brief outline of the TDM method [20,21]. In Sec. III we describe our calculations and present our results and comparison with others.

II. THE METHOD

The states and energies are obtained by diagonalizing the Hamiltonian

$$H = H_0 + V, \tag{1}$$

where (in atomic units)

$$H_0 = H_1 + H_2 + H_3 = \sum_{i=1}^{3} \left[-\frac{1}{2}\nabla_i^2 + \frac{Z}{r_i} \right]$$

and

$$V = \sum_{i<j} \frac{1}{r_{ij}} \tag{2}$$

using antisymmetric basis functions $\Psi(n_1 l_1, n_2 l_2, n_3 l_3; LS)$ constructed from single-particle wave functions. The totally antisymmetric three-electron wave function is expressed in terms of vector-coupled products of all antisymmmetric two-electron wave functions, $\phi_j(1,2|L_j S_j)$, constructed from two of the same three orbitals, and multiplied by the wave function of the third electron. That is,

$$\Psi_i(1,2,3) = \sum_j a_{ij} [\phi_j(1,2|L_j S_j)\varphi_j(3)]^{LS}$$

$$= \sum_j a_{ij} \Phi_j(1,2;3), \tag{3}$$

where $\varphi_j(r) = R_{nl}(r) Y_l^m(\theta,\phi)\chi_{1/2}^{\mu}$. The radial functions satisfy the orthogonality relation

$$\int_0^\infty R_{nl}(r) R_{nl'}(r) r^2 dr = \delta_{nn'}, \tag{4}$$

but are otherwise unspecified. We could, for example, use the generalized Laguerre functions

$$R_{nl}(r) = (2\lambda)^{3/2} \sqrt{\frac{(n-l-1)!}{(n+l+1)!}}\, e^{-\lambda r} (2\lambda r)^l L_{n-l-1}^{2l+2}(2\lambda r), \tag{5}$$

which constitute a complete set of normalizable functions as a basis set. However, in this work we use hydrogenic functions as we have found them to yield more accurate results for the higher levels in a Rydberg series.

The Ψ_i's are fully antisymmetric, while Φ_j is antisymmetric only in variables 1 and 2. The a_{ij} are generalized fractional-parentage coefficients (CFP). They make the linear combination fully antisymmetric in all variables. There may be more than one Ψ_i with the same set of orbitals and the same L, S, and π. If so, then a seniority index must be assigned to each of the independent functions. Hence the subscript $i = 1,2,\ldots$.

The energies are obtained by calculating (in blocks) and diagonalizing a matrix written symbolically as

$$H = \mathcal{A}\mathcal{H}\mathcal{A}^T, \tag{6}$$

where $\mathcal{A}$ is the matrix of the a_{ij}, $\mathcal{A}^T$ is its transpose, and $\mathcal{H}$ is the matrix whose components are given by

$$(\mathcal{H})_{ij} = \langle \Phi_i(1,2;3) | 3\left(H_3 + \frac{1}{r_{12}} \right) | \Phi_j(1,2:3) \rangle. \tag{7}$$

In this way, the two-electron interactions can be calculated in terms of

$$\langle \phi_i(1,2|n_1 l_1, n_2 l_2 : L_i S_i) | \frac{1}{r_{12}} | \phi_j(1,2|n_3 l_3, n_4 l_4 : L_j S_j) \rangle, \tag{8}$$

i.e., exactly the matrix elements used in the two-electron problem. (Of course, these terms are 0 unless $L_i = L_j$ and $S_i = S_j$.)

III. THE CALCULATION

The basis set used in the calculation includes all configurations of the form $n_1 l_1, n_2 l_2, n_3 l_3$, where $0 \leqslant l_i \leqslant l_{\max} = 5$ and $n_i \leqslant n_{\max} = 20$, with the following restrictions. Only if two of the three n_i are less than or equal to 3 can the third be as large as $n_{\max}$. Otherwise the maximum value is 6. Fur-

thermore, none of the n_i can equal 1, i.e., all the singly and doubly excited configurations are excluded. This latter restriction has been translated into projection-operator terminology [21] where the operators P, Q_I, Q_{II} project onto subspaces containing 0, 1, and 2 vacancies and where the eigenvalues of the operator $Q_{II}HQ_{II}$ are the energy levels of the hollow atomic states with double-*K*-shell vacancies.

This procedure yields different numbers of configurations depending on the particular L, S,π under consideration. For example, for the $^2S^o$ symmetry this procedure yields 183 configurations, while for $^2P^o$ the number is 671. Each configuration, in turn, produces anywhere from 0 to 10 antisymmetric basis functions, Ψ_i. The computer automatically generates the (orthonormal) basis functions for each given configuration, and evaluates the Hamiltonian matrix using all the previously mentioned basis functions generated for each and every configuration. This total number of basis functions is in general considerably larger than the number of configurations included in the calculation for the particular L, S, π symmetry. For example, for $^2S^o$ symmetry, the number of states is 260, while for $^2P^o$ the number is 1666. The Hamiltonian matrix is then diagonalized, yielding its eigenvalues (E_n) and eigenvectors (u_n). The energy levels so obtained are analyzed and fitted to one or more Rydberg series of the form

$$E[n_1 l_1 n_2 l_2 L_{12} S_{12} n l_3] = E[n_1 l_1 n_2 l_2 L_{12} S_{12}] - \frac{1}{2}\left(\frac{Z-2}{n^*}\right)^2, \tag{9}$$

where n^* is the effective quantum number and $E[n_1 l_1 n_2 l_2 L_{12} S_{12}]$ is the energy of a low-lying doubly excited state (in this paper, both electrons are in the $n_i=2$ state) of the Li^+ ion. For full details, see [20] and [21].

The quantum defect (μ_n), defined as $n-n^*$, is usually a slowly varying function of n when n is large, particularly in the case of a single isolated Rydberg series such as the $(2p)^2\,{}^3P^e np\,{}^2S^o$ series converging on the doubly excited $(2p)^2\,{}^3P^e$ state of the residual ion. This is demonstrated in Table III below and the attendant discussion. However, a Rydberg series of states can be perturbed by an isolated state from another series converging on a higher threshold. This causes the quantum defect, or equivalently, the effective quantum number, to deviate from the smooth behavior we expect for an isolated series of resonances. In such cases, more information is needed for identification, including a description of the wave functions. A specific example of this is presented in Table IV, Figs. 1–3, and associated discussion.

If for a particular L, S, π symmetry, such as, for example, $^2P^e$, there are multiple Rydberg series converging on a particular threshold (see Table I), the different series may strongly interact and actually cross. Then identification of the energy levels by their effective quantum number alone may not be possible, since in this case the levels are severely perturbed and the configuration mixings characteristic of each series are dramatically altered. A detailed example is given in Table IV, Fig. 3, and surrounding discussion.

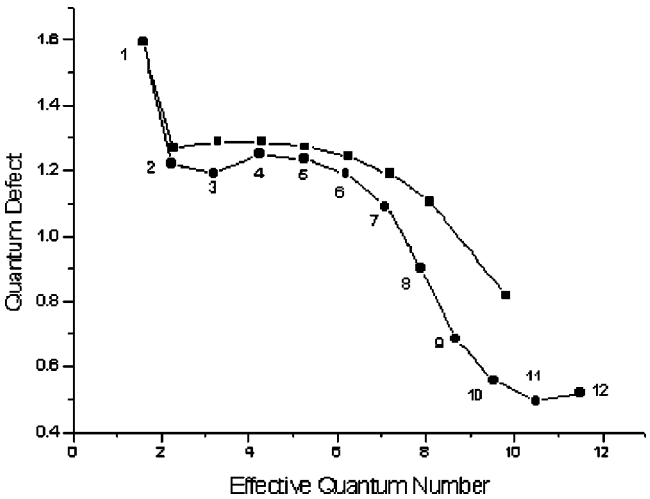

FIG. 1. Quantum defect vs effective quantum number for $\langle B, np\,{}^2P^e\rangle$ series including comparison with BN. The circles are from Table IV. State 8 is classified as $\langle C,3s\rangle$ (see Fig. 2 and discussion in text). Note that the BN values agree very well with ours, even as to the rapid drop of μ_n, and a ''missing'' state at $n^*\approx 9$ corresponding to our state 8.

The contributions of the various series to the normalization of the wave function for a particular energy level are evaluated by the following sums:

$$C(n_1 l_1 n_2 l_2 L_{12} S_{12} l_3) := \sum_n |u(n_1 l_1 n_2 l_2 L_{12} S_{12} n l_3)|^2, \tag{10}$$

where the u's are the elements of the eigenvector of the Hamiltonian matrix. Using these sets of numbers, the Rydberg series to which a particular energy level belongs can almost always be unambiguously determined, since these sets characterize each series.

In Table I, for the L, S, π symmetries discussed in this paper, we list the Rydberg-like series of energy levels con-

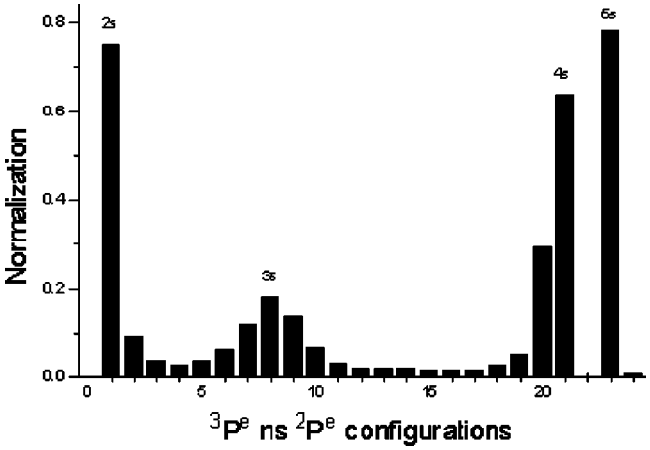

FIG. 2. Fraction of $\langle C,ns\rangle$ configurations in the lowest 24 levels of $^2P^e$. The $2s(2p)^2$ configuration is included in state 1. The sum of C_{ns} configurations from state 3 to state 17 is ≈ 0.92. This is a typical example of an isolated state embedded in a Rydberg series.

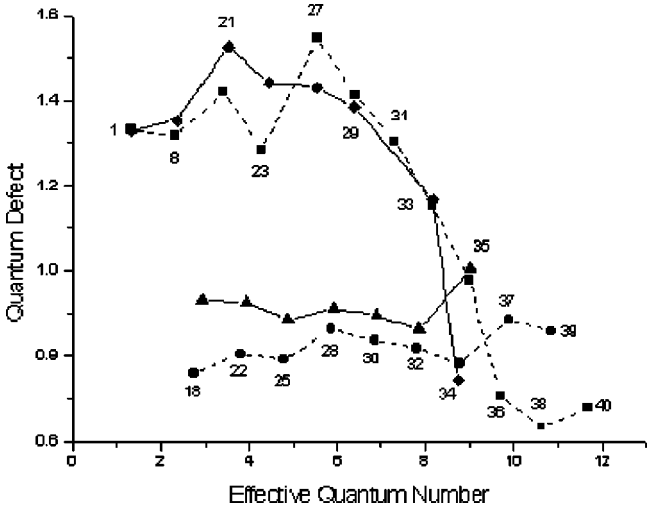

FIG. 3. $(1-\mu_n)$ versus n^* for C_{ns} and C_{nd} series with $^2P^e$ symmetry. Dashed lines (squares and circles) and numbers are from Table IV. Solid lines (diamonds and triangles) are from BN. Both we and BN show the two series crossing at $n^* \approx 9$. There are ''isolated'' states between 18 and 21 ($\langle E,3p\rangle$ at no. 20) and between 23 and 25 ($\langle D,3d\rangle$ at no. 24). We also have two spurious states (nos. 19 and 26).

verging on the doubly excited states of the residual ion, Li^+, as well as the energies (in a.u.) of these states. The threshold energies presented in the table are as follows. $E_1(I)$: These have been calculated using the TDM method for two-electron systems [22]; $E_2(I)$: These have been fitted to the series so that Eq. (9) yields the most consistent and smoothly varying effective quantum number n^* for all series and all symmetries. Details for the fitting procedure are given in [21].

Because we are discussing so many configurations and series, the standard notation is cumbersome. Therefore, we will often replace the two-electron target single-particle descriptions, $2l_1 2l_2\,^{1,3}L^\pi$, with a capital letter $I = A,B,C,D,E,F$, as shown in Table I. The independent-particle notation actually fails for thresholds marked A and F. It is well known from work done over 20 years ago that the lowest two doubly excited states of Li^+ with $^1S^e$ symmetry [labeled as $(2,2a)$ and $(2,2b)$ in [22]] are best described as

$$(2,2a) = \sqrt{a}(2s)^2 + \sqrt{1-a}(2p)^2$$

and

$$(2,2b) = \sqrt{1-a}(2s)^2 - \sqrt{a}(2p)^2, \tag{11}$$

respectively. Conneely and Lipsky [17] found that $a = 0.65$. This clearly carries over for three-electron systems, as is discussed in Sec. III B.

Our notation is completed by appending the quantum number and angular momentum of the third electron and enclosing both in the brackets $\langle\ \rangle$. If necessary, the total angular momentum and spin are included. Thus, e.g.,

$$\langle B,nd^2P^o\rangle := (2s2p)^3P^o nd^2P^o.$$

When there are two or more series converging to the same threshold, a further notational contraction is used in the tables, to describe the configuration mixings of the states. For instance, the sum in Eq. (10) for $n_1l_1 = 2s$, $n_2l_2 = 2p$, $L_{12} = P$, $S_{12} = 1$, and $l_3 = d$ is shortened to

$$\%B_d := C(2s2p\,^3P^o d) \times 100 = \sum_n |u(\langle B,nd\rangle)|^2 \times 100.$$

In view of the fact that the doubly excited thresholds are of the utmost importance in calculating n^*'s and so determining the Rydberg series to which the levels belong, we tabulate some recent experimental and theoretical values and compare them with the values obtained with the TDM method [22] in Table II. The energies are presented in eV (27.211 396 eV = 1 a.u.) above the neutral lithium ground state and in converting our TDM values we have used the experimental value of $-7.478\,060\,34$ a.u. quoted by McKenzie and Drake [26]. Figures in brackets are estimated uncertainties in the final digits of the experimental values.

It is seen from Table II that the lowest two thresholds, i.e., the $(2s)^2\,^1S^e$ and $(2s2p)\,^3P^o$ thresholds, are in reasonable agreement with other theoretical calculations and with experiment. There is less experimental data available for the the next threshold, the $(2p)^2\,^3P^e$ doubly excited state of Li^+, as this is a nonautoionizing state. However, the experimental value of -1.7908 a.u. (154.758 eV) of Buchet *et al.* [28] as quoted by Anderson *et al.* [29] is in excellent agreement with the value of $-1.790\,955$ (154.755 eV) obtained using the TDM method. Our next two thresholds are about 0.25 eV above the experimental value and the accurate results of

TABLE I. Lowest doubly excited thresholds and series classifications.

Threshold: $I=$	$(2s)^2\,^1S^e$ $\langle A\rangle$	$(2s2p)\,^3P^o$ $\langle B\rangle$	$(2p)^2\,^3P^e$ $\langle C\rangle$	$(2p)^2\,^1D^e$ $\langle D\rangle$	$(2s2p)\,^1P^o$ $\langle E\rangle$	$(2p)^2\,^1S^e$ $\langle F\rangle$
$E_1(I)$	-1.902344	-1.874873	-1.790955	-1.761243	-1.747782	-1.614321
$E_2(I)$	-1.89783	-1.87028	-1.78515	-1.75230	-1.73925	-1.60265
$^2S^o$			*np*			
$^2S^e$	*ns*	*np*		*nd*	*np*	*ns*
$^2P^o$	*np*	*ns,nd*	*np*	*np,nf*	*ns,nd*	*np*
$^2P^e$		*np*	*ns,nd*	*nd*	*np*	
$^2D^e$	*nd*	*np,nf*	*nd*	*ns,nd,ng*	*np,nf*	*nd*

TABLE II. Comparison (in eV) of the six lowest doubly excited Li^+ states (figures in parentheses are estimated uncertainties in the final digits).

Config.		Theory				Expt.		
		$E_1(I)$	$E_2(I)$	[23]	[24]	[27]	[9]	[19]
$(2s)^2\,{}^1S^e$	*A*	151.724	151.847	151.526	151.343	151.63	151.66(3)	151.68(10)
$(2s2p)\,{}^3P^o$	*B*	152.472	152.579	152.394	152.182	152.38	152.41(2)	152.41(10)
$(2p)^2\,{}^3P^e$	*C*	154.755	154.913	154.634	154.441	154.60		
$(2p)^2\,{}^1D^e$	*D*	155.563	155.807	155.370	155.215	155.31	155.33(2)	155.35(10)
$(2s2p)\,{}^1P^o$	*E*	155.930	156.162	155.732	155.520	155.67	155.71(2)	155.71(10)
$(2p)^2\,{}^1S^e$	*F*	159.562	159.879	159.291	159.175	159.13	159.16(3)	159.16(10)

Chung [27], but the $(2p)^2\,{}^1S^e$ threshold is fully 0.4 eV above the experimental and theoretical results.

The threshold energy shifts from $E_1(I)$ and $E_2(I)$, which are positive in all cases, have been discussed in Ref. [21], where it is argued that they are a consequence of the fact that only bound-state hydrogenic functions are used in the calculations.

To demonstrate how the n^*'s vary smoothy in the absence of another perturbing series, we present in Table III the single $(2p)^2\,{}^3P^e np\,{}^2S^o$ (or $\langle C_p\,{}^2S^o\rangle$) series, where we use the shifted $(2p)^2\,{}^3P^e$ energy of $-1.785\,15$ a.u. to calculate the effective quantum number. We note that since a $(2p)^3\,{}^2S^o$ term does not exist, the first member of the series must have $n=3$, and the quantum defect is effectively constant for the series. Furthermore, we see that when n^* exceeds 12, the μ_n's become erratic and consequently the last two states in Table III should be rejected. Hereafter, we will reject all states with $n^*>12$, and most with $n^*>11$. The wave function for each member of this series consists mainly ($\approx$94%) of configurations of the type $(2p)^2\,{}^3Pnp$, with very little contributions from any other configurations. That is to say, for each $\langle C,np\rangle$ the wave-function description is 94% C_p (or simply 94%C, since there is only one series).

We have relied heavily on n^*'s for classifying and comparing states with other calculations, particularly with BN. In [23] they calculate n^* relative to the nearest threshold below which each state lies, whereas the true n^* should be calculated relative to the threshold to which that series converges. We have used the following formula to convert their n^*'s. Let n_1^* be the effective quantum number as reported by BN. Let $E_2(J)$ be the energy of the nearest threshold, *J*, and $E_2(I)$ be the correct threshold, *I*. Then

$$n_2^*=\frac{1}{\sqrt{[2\Delta_{IJ}+1/(n_1^*)^2]}}, \tag{12}$$

where $\Delta_{IJ}=E_2(I)-E_2(J)$, and n_2^* is the ''correct'' n^*. In all cases we have used our values, as given in Table I, for the thresholds. In effect, we have scaled all their calculations to agree with our thresholds, $E_2(I)$. Given that these values come from the fitting of the n^*'s, there is a complete self-consistancy of our calculations. With this scaling understood, overall agreement between their results and ours is very good indeed. We make a detailed comparison of the two sets of calculations for series with $^2P^e$ symmetry in the following subsection.

TABLE III. Energy and n^* for $(2p)^2\,{}^3P^e\,np\,{}^2S^o$ series in Li.

n	$-E$ (a.u.)	n^*
3	1.883344	2.25654
4	1.832756	3.24081
5	1.811926	4.32132
6	1.802685	5.33987
7	1.797565	6.34628
8	1.794411	7.34774
9	1.792328	8.34628
10	1.790878	9.34264
11	1.789829	10.33726
12	1.789017	11.37064
13	1.788122	12.97118
14	1.786708	17.91545

A. The series with $^2P^e$ symmetry

Although there is very little experimental data on hollow states with $^2P^e$ symmetry, our analysis shows several interesting characteristics which are important for understanding symmetries with multiple series.

From Table I we see there are five series with this symmetry. Independent-particle nomenclature would describe a typical level as $2s2p^3P^onp$, which we call $\langle B,np\rangle$. We label the other four series as $\langle C,ns\rangle$, $\langle C,nd\rangle$, $\langle D,nd\rangle$, and $\langle E,np\rangle$. Whereas the $\langle C,np^2S^o\rangle$ series described in Table III above was a perfect example of a noninteracting series with almost constant quantum defects, the $^2P^e$ symmetry yields good examples of the following.

(i) A single state that is the first member of three series. The first state, i.e., the $2s(2p)^2$ state, is the lowest level of each of $\langle B,np\rangle$, $\langle C,ns\rangle$, and $\langle E,np\rangle$, with $n=2$. That is to say, the state can be described as $(2s2p)\,{}^3P^o2p$ or $(2p)^2\,{}^3P^e2s$ or $(2s2p)^1P^o2p$. This is because whether we couple a $2s$ electron to an antisymmetric $(2p)^2\,{}^3P^e$ wave function and antisymmetrize to give a wave function of $^2P^e$ symmetry, or couple a $2p$ electron with an antisymmetric $(2s2p)\,{}^{1,3}P^o$ wave function, and then antisymmetrize and normalize, we get the same function.

TABLE IV. Energies, n^*, and classification of $^2P^e$ states of Li.

No.	Config.	Energy	n^*	Description
1	$2s(2p)^2$ [a]	2.067462	1.59240	19%E 13%C_s 5%B 54%$2s(2p)^2$
2	$\langle B,3p\rangle$	1.971677	2.22061	85%B 9%C_s
3	$\langle B,4p\rangle$	1.919282	3.19432	92%B
4	$\langle B,5p\rangle$	1.897988	4.24795	93%B 3%C_s
$\langle A\rangle$	Threshold	1.897830		
5	$\langle B,6p\rangle$	1.888525	5.23502	92%B 4%C_s
6	$\langle B,7p\rangle$	1.883328	6.19033	89%B 6%C_s
7	$\langle B,8p\rangle$	1.880226	7.09042	82%B 11%C_s
8	$\langle C,3s\rangle$	1.878293	2.31692	74%B 18%C_s
9	$\langle B,9p\rangle$	1.876908	8.68568	80%B 14%C_s
10	$\langle B,10p\rangle$	1.875754	9.55729	88%B 6%C_s
11	$\langle B,11p\rangle$	1.874819	10.49543	92%B 3%C_s
12	$\langle B,12p\rangle$	1.874048	11.51875	94%B
$\langle B\rangle$	Threshold	1.870280		
18	$\langle C,3d\rangle$	1.849150	2.79508	79%C_d 3%C_s 8%B
20	$\langle E,3p\rangle$	1.841264	2.21389	41%E 30%C_s 14%D 6%C_d
21	$\langle C,4s\rangle$	1.827940	3.41835	64%C_s 13%E 10%B 6%D
22	$\langle C,4d\rangle$	1.819696	3.80438	91%C_d
23	$\langle C,5s\rangle$	1.812375	4.28553	78%C_s 14%B
24	$\langle D,3d\rangle$	1.807407	3.01217	45%C_d 33%D 13%E
25	$\langle C,5d\rangle$	1.806938	4.79042	33%C_d 29%D 20%B 6%C_s
27	$\langle C,6s\rangle$	1.801403	5.54644	57%C_s 17%C_d 14%B 5%E
28	$\langle C,6d\rangle$	1.799700	5.86215	77%C_d 14%C_s 3%B
29	$\langle C,7s\rangle$	1.797314	6.41139	75%C_s 5%E 3%B 9%C_d
30	$\langle C,7d\rangle$	1.795842	6.83840	83%C_d 10%C_s
31	$\langle C,8s\rangle$	1.794524	7.30350	73%C_s 7%E 10%C_d 3%D
32	$\langle C,8d\rangle$	1.793327	7.81977	77%C_d 15%C_s
33	$\langle C,9s\rangle$	1.792674	8.15188	61%C_s 9%E 16%C_d 5%D
34	$\langle C,9d\rangle$	1.791633	8.78225	52%C_d 37%C_s 2%D 3%E
35	$\langle C,10s\rangle$	1.791353	8.97816	41%C_d 40%C_s 7%E 4%D
36	$\langle C,11s\rangle$	1.790458	9.70544	73%C_s 14%C_d 3%D 3%E
37	$\langle C,10d\rangle$	1.790266	9.88551	79%C_d 12%C_s 2%E
38	$\langle C,12s\rangle$	1.798571	10.63469	86%C_s 2%D 3%C_d 3%E
39	$\langle C,11d\rangle$	1.789391	10.85773	90%C_d 3%C_s
$\langle C\rangle$	Threshold	1.785150		
48	$\langle D,4d\rangle$	1.780457	4.21398	59%C_s 27%D 5%E
49	$\langle E,4p\rangle$	1.778772	3.55686	20%E 33%C_s 23%D 14%C_d
52	$\langle D,5d\rangle$	1.771809	5.06256	55%D 29%C_s 4%E 2%C_d
54	$\langle D,6d\rangle$	1.766470	5.94027	56%D 23%E 4%C_s 5%C_d
55	$\langle E,5p\rangle$	1.763686	4.52343	52%D 31%E 5%C_s
56	$\langle D,7d\rangle$	1.761292	7.45678	73%D 14%E
57	$\langle D,8d\rangle$	1.759251	8.48149	76%D 10%E
58	$\langle D,9d\rangle$	1.757837	9.50305	64%D 17%E 7%C_s
59	$\langle D,10d\rangle$	1.756949	10.37115	56%D 15%E 17%C_s
60	$\langle D,11d\rangle$	1.756136	11.41710	75%D 10%C_s 3%E
63	$\langle E,6p\rangle$	1.753941	5.83388	44%E 25%C_s 20%D
$\langle D\rangle$	Threshold	1.752300		
66	$\langle E,7p\rangle$	1.750105	6.78652	52%E 30%D 4%C_s 1%C_d
69	$\langle E,8p\rangle$	1.747032	8.01554	73% 13%D 1%C_s
70	$\langle E,9p\rangle$	1.745295	9.09502	76%E 10%D
71	$\langle E,10p\rangle$	1.744127	10.12562	62%E 24%D 24%C_d
72	$\langle E,11p\rangle$	1.743351	11.04228	61%E 25%D 1%C_d
$\langle E\rangle$	Threshold	1.739250		

[a]Level no. 1 is the first member of three series $\langle B,2p\rangle$,$\langle C,2s\rangle$,$\langle E,2p\rangle$.

(ii) Extensive configuration mixings. It is clear from Table IV that most of these states cannot be described by a single configuration. Indeed it is seen that each state is a mixture of configurations, so we present the percentage each series contributes to the normalization of each state.

(iii) A single series interacting with an isolated state. ($\langle B, np\rangle$ series interacts with the $\langle C,3s\rangle$ state).

(iv) Two series converging to the same threshold, crossing each other. ($\langle C,ns\rangle$ and $\langle C,nd\rangle$ series cross at $n\approx 9$.)

The last item also includes interactions with two spurious states (no. 19, a $\langle B,np\rangle$ state that lies above its threshold, and another one, no. 26, that defies classification) that are not true states. There are also two isolated states, the $\langle E,3p\rangle$ state at no. 20 and the $\langle D,3d\rangle$ state at no. 24, that interact mostly with the $\langle C,ns\rangle$ series. These are discussed fully, and compared with BN in Figs. 1–3 and the surrounding material. Our energy and classification results are tabulated in Table IV.

1. The $\langle B\rangle$ series—interacting with an isolated ($\langle C,3s\rangle$) state

Because different series converge to thresholds with different energies, the lowest members of one series may lie in the energy range just below the threshold of another series. Then we have what Fano [15] calls an isolated state interacting with a Rydberg series. This is clearly what is occurring between the $\langle B,np\,^2P^e\rangle$ series and the $\langle C,3s\rangle$ state. (This is the second lowest member of the $\langle C,ns\rangle$ series, since state no. 1 is the lowest member of three series.) This might best be understood by first discussing the corresponding, but more familiar, results for open-channel phase shifts. In the latter theory (see, e.g., [15]) one looks for resonances in electron scattering by looking for rapid changes by π in the phase shift. The same phenomenon occurs for closed channels, with $\pi\mu_n$ replacing the phase shift. This is demonstrated quite clearly in Fig. 1, where $1-\mu_n$ is plotted against n^*. The circles and the numbers are those given in Table IV. The μ_n's, rather than being slowly varying, as in Table III, rapidly change from 1.6 to 0.6, a change of one whole unit. This change corresponds to having one too many states in the series, indicating that there is a state from another series mixing in. We have identified state no. 8 as the extra state. But such an identification is somewhat arbitrary, since what would have been the $\langle C,3s\rangle$ state interacts strongly with several members of the $\langle B,np\rangle$ series.

Before discussing this further, note that we have also plotted the values taken from BN. The agreement between the two sets of calculations is very good, particularly as to the rapid change of μ_n. However, they have classified their highest member, which agrees closely with our state no. 10, as the $\langle C,3s\rangle$ state. It might be informative if they looked more closely in this region, particularly since their widths are actually getting broader with increasing n, instead of narrowing according to $(1/n^*)^3$. Such broadenings usually indicate interactions with other channels or series.

To show how difficult it is to uniquely identify the $\langle C,3s\rangle$ state, we have plotted the percent of $(2p)^2\,^3P^e ns$ configurations in each of the states numbered 1 through 24 in Fig. 2. Most of these correspond to members of the $\langle B\rangle$ series, including several spurious ones [15–17,19] that lie above the $\langle B\rangle$ threshold. State no. 1 is actually 54% $2s(2p)^2$, and so can be identified as the $\langle C,2s\rangle$ as well as the $\langle B,2p\rangle$ or $\langle E,2p\rangle$ states. At the other end, state no. 23 is clearly the $\langle C,5s\rangle$, while either no. 20 or more likely no. 21 is the $\langle C,4s\rangle$ state. No state from no. 3 to no. 19 has as much as 20% $\langle C,ns\rangle$ in it. Yet the sum over all those states is >0.92. Therefore, the $\langle C,3s\rangle$ state is in there somewhere. For obvious reasons, we have identified it with state no. 8.

2. The $\langle C,ns\rangle$ and $\langle C,nd\rangle$ series—crossing series

In this subsection we look at the energy region between the $\langle B\rangle$ and $\langle C\rangle$ thresholds. For completeness, we have also included states no. 1 and no. 8 in Fig. 3 that also appeared in Fig. 1. The n^*'s used in the two figures for these two levels are related by Eq. (12). The quantum defect structure is far more complex here than in the preceding section, as there are two series converging to the $\langle C\rangle$ threshold. In addition, there are two isolated states from higher series (no. 20, $\langle E,3p\rangle$ and no. 24, $\langle D,3d\rangle$) interacting with these series, and unfortunately for us, two spurious states (nos. 19 and 26).

The numbers and dashed lines in Fig. 3 correspond to our calculations in Table IV. We have also plotted the corresponding results from BN [with the two lowest states transformed by Eq. (12)]. As in Fig. 1, agreement is very good, particularly the rapid change in $\mu_n(C_s)$, and the series crossing.

It should be understood that if the series are classified according to their wave functions, they actually do cross, in apparent contradiction to phase shift or perturbation theory analysis. To understand this, we again first describe the corresponding behavior for two interacting open channels. In that case, it is well known that the phase shifts for the two channels will first approach and then diverge from each other as a function of increasing energy, just as two branches of a hyperbola do. What is less well known is that the wave-function characteristics corresponding to the two channels do cross. Suppose, for instance, that $\langle C,ks\rangle$ and $\langle C,kd\rangle$ are open channels corresponding to s and d electrons scattering off a $\langle C\rangle$ target. Suppose further that the phase shift for the s channel lies above the d channel when the energy is well below the noncrossing region. Then as the energy (or wave number k) is increased, the wave functions will mix, and finally, for energy well above the noncrossing region, the phase shift for the s channel will lie below the d channel. The same occurs for a closed channel or quantum defect behavior. The difference is, of course, that we are now dealing with a finite set of points, not a pair of continuous curves in the region of interaction, so the word crossing is not fully appropriate.

Unlike our discussion of Fig. 1, we cannot give a simple explanation of the rapid change in $\mu_n(C_s)$, since the two isolated states (20 and 24) and the two spurious states all lie below $n^*=5$. A more detailed analysis is necessary. However, the sum of the contributions of $\langle B\rangle$, $\langle D\rangle$, and $\langle E\rangle$ states to all the $\langle C,nl\rangle$ states between 27 and 39 comes to over 0.80, so there is something there, perhaps an extra smeared out state.

At this point it is appropriate to discuss spurious states in more detail. In the TDM method, we include all states of a given configuration up to some maximum $n_{\max}$ (in this paper, $n_{\max}=20$). In any diagonalization procedure, the trace (sum of diagonal elements) stays constant. Each diagonal element of H_{ii} from Eq. (1) can be thought of as a one-state approximation of that state's energy. After diagonalization, many of the elements will be much lower, some corresponding to physical values as quoted here. But since the trace remains unchanged, some other values will be much higher than before, even above threshold. This has been discussed in detail before (see e.g., [17,21,22]). But here, those spurious levels that lie above their appropriate threshold can interfere with states that appropriately lie in that range, as in this case, where levels 19 and 26 could actually be pushing up levels 21 and 27. Such effects should not be perceived of as being physical. That is, the true curve for $\mu_n(C_s)$ for $n=3,4,\ldots,8$ is almost surely smoother than the upper dotted curve in Fig. 3. Of course, the interference due to states 20 and 24 is real. However, the effects due to spurious states are not all imaginary. They do indicate to what extent the open $\langle B,kp\rangle$ channel couples to the $\langle C,ns\rangle$ and $\langle C,nd\rangle$ series. If the coupling is large enough, then there should be some experimental evidence for autoionization through the process

$$\langle C,nl\rangle \rightarrow \langle B\rangle + e^-(kl'),$$

i.e.,

$$\mathrm{Li}[(2p)^2 {}^3P^e nl] \rightarrow \mathrm{Li}^+[2s2p^3P^0] + e^-(kl').$$

As far as we know, no one has looked for such resonant structure in the electron energy range (from Table II) of 0 to $154.913-152.579=2.334$ eV (the difference between the $\langle B\rangle$ and $\langle C\rangle$ thresholds).

B. The series with $^2P^o$ symmetry

It is for the $^2P^0$ triply excited states of the lithium atom that most experimental and theoretical data exist. This is because investigations of hollow lithium states have, in the main, been restricted to excitation from the ground $(1s)^2 2s^2 S^e$ state, and the dipole selection rules allow only the formation of the $^2P^o$ states. Here, as can be seen from Table I, we have nine Rydberg series converging on the doubly excited states of Li^+. We label these series in the following manner:

$\langle A\rangle$	$(2s)^2 {}^1S^e np,$	$\langle F\rangle$	$(2p)^2 {}^1S^e np,$	$\langle B_s\rangle$	$(2s2p)\,{}^3P^o ns,$
$\langle B_d\rangle$	$(2s2p)\,{}^3P^o nd,$	$\langle C\rangle$	$(2p)^2 {}^3P^e np,$	$\langle D_p\rangle$	$(2p)^2 {}^1D^e np,$
$\langle D_f\rangle$	$(2p)^2 {}^1D^e nf,$	$\langle E_s\rangle$	$(2s2p)\,{}^1P^o ns,$	$\langle E_d\rangle$	$(2s2p)\,{}^1P^o nd.$

As noted previously in Eq. (11), and as discussed below, the $\langle A\rangle$ and $\langle F\rangle$ series are not properly defined by independent electron notation.

In Table V we present our classification of the triply excited states together with the energies (in a.u.) and the n^*'s, with a description of each state. As explained above, the n^* for these states is based not on the calculated two-electron doubly excited thresholds, but on the shifted threshold energies computed to give a good fit. It should be emphasized that the same shifted threshold energy is used for all $^{2S+1}L^\pi$ configurations [21].

It is clear from Table V, as was the case with Table IV, that most of these states cannot be described by a single configuration. As is seen from the table, considerable, apparently random, mixings occur when states of different series are close in energy. However, especially close to thresholds where there is no interference from other series, the mixings which describe a particular series are very stable and consistent. For example, the $\langle A,np\rangle$ series of states converge on the $\langle A\rangle$ threshold [see Eq. (11)] and below that threshold the states are described, with remarkable consistency, as being 73% $\langle A,np\rangle$ and 23% $\langle F,np\rangle\,[(2p)^2 {}^1S^e\,np]$. A very similar pattern occurs for the $\langle F,np\rangle$ series where the states are described as being 21% $\langle A,np\rangle$ and 61% $\langle F,np\rangle\,[(2p)^2 {}^1S^e\,np]$. Both of these mixings agree strongly with the idea that the outer electron sees a $(2,2a)$ or $(2,2b)$ core as described in Eq. (11). This mixing also occurs for the $^2D^e$ and $^2S^e$ symmetries (see below). This point of view was first presented in Ahmed and Lipsky [20], but their basis set was much too small to demonstrate anything. One interesting thought that may deserve further investigation is the fact that the two-electron calculations of [22] strongly indicate a mixing ratio of 2:1, but the three-electron calculations presented here indicate a somewhat different, 3:1 ratio. This may indicate that the outer electron slightly distorts the core.

Similar to Table IV, we note that the state with the lowest energy, i.e., $E_n=-2.242\,801$, is common to series $\langle A_p\rangle$, $\langle B_s\rangle$, and $\langle E_s\rangle$. That is to say, the state can be described as $(2s)^2 {}^1S^e\,2p$ or $(2s2p)^3P^o\,2s$ or $(2s2p)^1P^o\,2s$. For the same reason, the second state in Table V with energy $E_n=-2.003\,494$ is the first member of three series $\langle F_s\rangle$, $\langle C_s\rangle$, and $\langle D_s\rangle$. It may be described as $(2p)^2 {}^3P^e\,2p$ or $(2p)^2 {}^1D^e\,2p$ or $(2p)^2 {}^1S^e\,2p$.

In Table VI we compare our results (TDM method) for the $^2P^o$ series with the results of Chung and Gou (saddle-point method) and the *R*-matrix calculations of BN and the results of Vo Ky *et al.* (*R*- matrix) and with experiment. In order to compare with experiment, we give our energies in eV above the Li $(1s)^2(2s^2S^e$ ground state which we have

TABLE V. Energies, n^*, and classification of $^2P^o$ states of Li.

No.	Config.	Energy	n^*	Description
1	$(2s)^2 2p$ [a]	2.242801	1.20391	72%A 11%F 10%B_s
2	$(2p)^3$ [b]	2.003494	1.11686	40%F 27%B_s 12%A
3	$(A,3p)$	1.987946	2.35550	60%A 25%F
4	$\langle B,3s\rangle$	1.965687	2.28926	64%B_s 14%A 9%C
5	$\langle A,4p\rangle$	1.942255	3.35484	69%A 22%F
6	$\langle B,3d\rangle$	1.927816	2.94792	85%B_d 7%B_s
7	$\langle A,5p\rangle$	1.924122	4.36091	64%A 27%F 7%B_s
8	$\langle B,4s\rangle$	1.918723	3.21268	66%B_s 18%A 6%F
9	$\langle A,6p\rangle$	1.914475	5.48072	67%A 22%F 8%B_s
10	$\langle A,7p\rangle$	1.909838	6.45291	72%A 22%F
11	$\langle A,8p\rangle$	1.906842	7.44856	72%A 23%F
12	$\langle A,9p\rangle$	1.904835	8.44874	73%A 23%F
13	$\langle A,10p\rangle$	1.903428	9.45064	73%A 23%F
14	$\langle A,11p\rangle$	1.902408	10.45018	72%A 23%F
15	$\langle B,4d\rangle$	1.901792	3.98331	75%B_d 11%A 6%B_s
19	$\langle B,5s\rangle$	1.897926	4.25271	58%B_s 25%A 8%F
$\langle A\rangle$	Threshold	1.897830		
22	$\langle B,5d\rangle$	1.890427	4.98172	90%B_d 5%B_s
23	$\langle B,6s\rangle$	1.888411	5.25136	81%B_s 7%A 6%B_d
25	$\langle B,6d\rangle$	1.884238	5.98520	92%B_d 3%B_s
26	$\langle B,7s\rangle$	1.882848	6.30747	85%B_s 6%A
27	$\langle B,7d\rangle$	1.880536	6.98234	91%B_d 5%B_s
28	$\langle B,8s\rangle$	1.879736	7.27151	89%B_s 5%B_d
29	$\langle B,8d\rangle$	1.878129	7.98160	90%B_d 6%B_s
30	$\langle B,9s\rangle$	1.877618	8.25434	89%B_s 6%B_d
31	$\langle B,9d\rangle$	1.876479	8.98076	89%B_d 7%B_s
32	$\langle B,10s\rangle$	1.876136	9.24026	88%B_s 7%B_d
33	$\langle B,10d\rangle$	1.875300	9.97974	89%B_d 8%B_s
34	$\langle B,11s\rangle$	1.875060	10.22724	88%B_s 8%B_d
35	$\langle B,11d\rangle$	1.874423	10.98585	88%B_d 8%B_s
36	$\langle B,12s\rangle$	1.874239	11.23879	86%B_s 8%B_d
$\langle B\rangle$	Threshold	1.870280		
45	$\langle E,3s\rangle$	1.866322	1.98362	30%E_s 23%A 23%D_p 6%C
49	$\langle C,3p\rangle$	1.856718	2.64318	49%B_s 38%C 3%E_s
53	$\langle C,4p\rangle$	1.826290	3.48620	36%B_d 32%C 9%D_p 7%E_s
55	$\langle D,3p\rangle$	1.820848	2.70077	40%C 28%D_p 10%E_s 4%B_s
56	$\langle C,5p\rangle$	1.810050	4.48107	60%C 25%E_d 5%E_s
57	$\langle E,3d\rangle$	1.807621	2.70427	44%E_d 24%C 7%D_f 5%A
58	$\langle C,6p\rangle$	1.802828	5.31821	45%C 22%D_p 18%E_s 4%B_s
59	$\langle E,4s\rangle$	1.802224	2.81777	29%B_s 21%D_p 19%E_s 14%C
60	$\langle C,7p\rangle$	1.798985	6.01165	68%C 20%B_s
61	$\langle C,8p\rangle$	1.795876	6.82761	84%C 6%B_s
62	$\langle C,9p\rangle$	1.793475	7.74990	89%C 3%B_s
63	$\langle C,10p\rangle$	1.791753	8.70160	90%C
64	$\langle C,11p\rangle$	1.790508	9.66049	91%C
65	$\langle C,12p\rangle$	1.789583	10.62013	91%C
$\langle C\rangle$	Threshold	1.785150		
70	$\langle D,4f\rangle$	1.784229	3.95722	72%D_f 10%C
73	$\langle D,4p\rangle$	1.776487	4.54669	59%D_p 17%C 11%E_s
74	$\langle E,4d\rangle$	1.775190	3.72988	65%E_d 10%C 9%D_f
75	$\langle D,5f\rangle$	1.771524	5.09993	79%D_f 4%C 5%E_d
76	$\langle D,5p\rangle$	1.769780	5.34821	52%D_p 30%C 5%E_s
77	$\langle E,5s\rangle$	1.768911	4.10573	41%C 32%E_s 12%D_p

TABLE V. (*Continued*).

No.	Config.	Energy	n^*	Description
78	$\langle D,6p\rangle$	1.765901	6.06321	$45\%D_p\ 33\%E_s\ 4\%B_d$
79	$\langle D,6f\rangle$	1.765192	6.22770	$86\%D_f\ 2\%E_d$
80	$\langle D,7p\rangle$	1.763212	6.76907	$65\%D_p\ 9\%E_s\ 8\%B_d$
81	$\langle D,7f\rangle$	1.761502	7.37131	$85\%D_f\ 3\%E_d$
82	$\langle D,8p\rangle$	1.760659	7.73408	$60\%D_p\ 14\%E_d\ 12\%B_d$
83	$\langle E,5d\rangle$	1.760573	4.84245	$67\%E_d\ 15\%D_p\ 5\%D_f$
84	$\langle D,8f\rangle$	1.759127	8.55769	$66\%D_f\ 11\%B_d\ 9\%D_p$
85	$\langle D,9p\rangle$	1.758856	8.73278	$40\%D_p\ 23\%B_d\ 3\%E_s$
86	$\langle E,6s\rangle$	1.758335	5.11841	$33\%E_s\ 39\%D_p\ 13\%B_d$
87	$\langle D,9f\rangle$	1.757407	9.89516	$87\%D_f$
88	$\langle D,10p\rangle$	1.757223	10.07765	$75\%D_p\ 12\%E_s$
89	$\langle D,10f\rangle$	1.756258	11.23997	$45\%D_f\ 37\%D_p$
97	$\langle E,6d\rangle$	1.753369	5.95084	$61\%E_d\ 25\%D_f\ 2\%C$
$\langle D\rangle$	Threshold	1.752300		
100	$\langle E,7s\rangle$	1.751321	6.43583	$50\%E_s\ 36\%D_p$
102	$\langle E,7d\rangle$	1.749282	7.05978	$74\%E_d\ 7\%D_p$
105	$\langle E,8s\rangle$	1.747884	7.60979	$45\%E_s\ 40\%D_p$
106	$\langle E,8d\rangle$	1.746517	8.29498	$81\%E_d\ 4\%D_p$
107	$\langle E,9s\rangle$	1.746077	8.55816	$68\%E_s\ 12\%D_p$
108	$\langle E,10s\rangle$	1.744863	9.43791	$40\%E_s\ 30\%E_d\ 15\%D_p$
109	$\langle E,9d\rangle$	1.744661	9.61266	$56\%E_d\ 21\%E_s\ 4\%D_f$
110	$\langle E,11s\rangle$	1.743889	10.38184	$46\%E_s\ 33\%D_f$
112	$\langle E,10d\rangle$	1.743395	10.98270	$75\%E_d\ 7\%D_f\ 5\%E_s$
$\langle E\rangle$	Threshold	1.739250		
134	$\langle F,3p\rangle$	1.692512	2.35884	$25\%F\ 19\%C\ 10\%D_p\ 11\%E_s$
139	$\langle F,4p\rangle$	1.647171	3.35121	$41\%F\ 10\%E_d\ 16\%A$
140	$\langle F,5p\rangle$	1.628527	4.39569	$60\%F\ 21\%A$
141	$\langle F,6p\rangle$	1.619681	5.41840	$60\%F\ 21\%A$
142	$\langle F,7p\rangle$	1.614742	6.43044	$61\%F\ 21\%A$
143	$\langle F,8p\rangle$	1.611683	7.43992	$61\%F\ 21\%A$
144	$\langle F,9p\rangle$	1.609654	8.44940	$61\%F\ 21\%A$
145	$\langle F,10p\rangle$	1.608237	9.45998	$61\%F\ 21\%A$
146	$\langle F,11p\rangle$	1.607209	10.47262	$61\%F\ 21\%A$
$\langle F\rangle$	Thresheld	1.602605		

[a]Level no. is the first member of three series: $\langle A,2p\rangle,\langle B,2s\rangle,\langle E,2s\rangle$.
[b]Level no. 2 is the first member of three series: $\langle C,2p\rangle,\langle D,2p\rangle,\langle F,2p\rangle$.

taken to be $-7.470\,976$ a.u. in order to give us exact agreement with the accurate calculation of Chung for the first member of the series. This effectively lowers all our energies by 0.2 eV.

As seen in Table VI, our classification agrees with that of Chung and Gou [13,14] in general except for the states $\langle B,3d\rangle$ and $\langle A,5p\rangle$, where they have them in reverse order. We note that BN and Vo Ky *et al.* agree with Chung's classification of these energy levels. However, Chung agrees with us with regard to the $\langle B,4s\rangle$ and the $\langle A,6p\rangle$ states, whereas BN and Vo Ky *et al.* have these states reversed. Our classifications agree with both BN and Vo Ky *et al.* in the energy range 151.3 eV to above the $\langle B\rangle$ threshold. There are, however, ambiguities in the classification of the first eight states in the energy region between the $\langle B\rangle$ and the $\langle C\rangle$ thresholds. As can be seen from Table V, these states are severely mixed. We have classified these states as $\langle E,3s\rangle,\langle C,3p\rangle,\langle C,4p\rangle,\langle D,3p\rangle,\langle C,5p\rangle,\langle E,3d\rangle,\langle C,6p\rangle,\langle E,4s\rangle$, whereas BN has classified them as $\langle E,3s\rangle,\langle C,3p\rangle,\langle D,3p\rangle,\langle C,4p\rangle,\langle E,3d\rangle,\langle C,5p\rangle,\langle E,4s\rangle,\langle C,6p\rangle$, and Vo Ky *et al.* have classified them as $\langle E,3s\rangle,\langle C,3p\rangle,\langle C,4p\rangle,\langle E,3d\rangle,\langle D,3p\rangle,\langle C,5p\rangle,\langle E,4s\rangle,\langle C,6p\rangle$.

From our point of view, the only questionable assignment is that of state number 55 in Table V, which we classify as $\langle D,3p\rangle$ despite its containing %40 C and only %28 D_p. However, the fact that the adjacent states can be unambiguously classified in terms of their configuration mixings and quantum defects leaves us with no choice in the matter short of an analysis which is much more complex than that given for Figs. 1–3 (five interacting series versus two or three interacting series).

We note that Vo Ky *et al.* give the same energy for the $\langle C,4p\rangle$ and $\langle E,3d\rangle$ states (153.35 eV) and also the $\langle E,4s\rangle$ and $\langle C,6p\rangle$ states (154.05 eV). We also note that above the

TABLE VI. Comparison of energies (in eV) for some triply excited $^2P^o$ states.

State	This work	Chung and Gou	*BN*	Vo Ky *et al.*	Expt. [5,12]	Expt. [3]	Expt. [2]
$(2s)^2 2p$	142.255	142.255	142.30	142.12	142.28	142.33	142.35
$(2p)^3$	148.766	148.729	148.81	148.68	148.77	148.7	
$\langle A,3p\rangle$	149.189	149.241	149.22	149.07			
$\langle B,3s\rangle$	149.795	149.846	149.86	149.69	149.95	149.91	149.79
$\langle A,4p\rangle$	150.432	150.480	150.40	150.24			
$\langle B,3d\rangle$	150.825	150.947	150.94	150.74			
$\langle A,5p\rangle$	150.926	150.917	150.84	150.67			
$\langle B,4s\rangle$	151.073	151.119	151.14	150.95	151.22	151.20	151.10
$\langle A,6p\rangle$	151.188	151.203	151.06	150.88			
$\langle A,7p\rangle$	151.315	151.349	151.21	151.03			
$\langle A,8p\rangle$	151.396	151.28	151.11				
$\langle A,9p\rangle$	151.451		151.34				
$\langle B,4d\rangle$	151.533		151.56	151.36			
$\langle B,5s\rangle$	151.639		151.66	151.45	151.68		
$\langle A\rangle$	Threshold						
$\langle B,5d\rangle$	151.843		151.86	151.63			
$\langle B,6s\rangle$	151.898		151.91	151.71	151.92		
$\langle B,6d\rangle$	152.011		152.02	151.82			
$\langle B,7s\rangle$	152.049		152.05	151.85	152.06		
$\langle B,7d\rangle$	152.112		152.12	151.92			
$\langle B,8s\rangle$	152.134		152.14	151.93	152.15		
$\langle B,8d\rangle$	152.177		152.18	151.98			
$\langle B,9s\rangle$	152.191		152.20	151.99			
$\langle B,9d\rangle$	152.222		152.23	152.02			
$\langle B\rangle$	Threshold						
$\langle E,3s\rangle$	152.499	152.453	152.45	152.32	152.90	152.75	152.32
$\langle C,3p\rangle$	152.760	152.742	152.76	152.57	152.51	152.46	152.72
$\langle C,4p\rangle$	153.588	153.572	153.70	153.35	153.66	153.54	153.43
$\langle D,3p\rangle$	153.736		153.53	153.52			
$\langle C,5p\rangle$	154.030		154.05	153.81			
$\langle E,3d\rangle$	154.096		153.99	153.35			
$\langle C,6p\rangle$	154.226		154.23	154.05			
$\langle E,4s\rangle$	154.243		154.15	154.05			
$\langle C,7p\rangle$	154.331		154.33	154.15			
$\langle C\rangle$	Threshold						
$\langle D,4f\rangle$	154.732		154.57				
$\langle D,4p\rangle$	154.943		154.48	153.97			
$\langle E,4d\rangle$	154.978		154.82	154.34			
$\langle D,5f\rangle$	155.078		154.85				
$\langle D,5p\rangle$	155.125		154.74	154.56			
$\langle E,5s\rangle$	155.149		154.90	154.75			
$\langle D,6p\rangle$	155.231		154.99	154.76			
$\langle D,6f\rangle$	155.250		155.50				
$\langle D,7p\rangle$	155.304		155.07	154.90			
$\langle D,7f\rangle$	155.351		155.10				
$\langle D,8p\rangle$	155.374		155.13	154.98			
$\langle E,5d\rangle$	155.376		155.15	154.83			
$\langle D,8f\rangle$	155.415		155.16				
$\langle D,9p\rangle$	155.423		155.18	155.03			
$\langle E,6s\rangle$	155.437		155.21	155.02			
$\langle D,9f\rangle$	155.462		155.21				
$\langle D,10p\rangle$	155.467			155.07			

TABLE VI. (*Continued*.)

State	This work	Chung and Gou	*BN*	Vo Ky *et al.*	Expt. [5, 12]	Expt. [3]	Expt. [2]
$\langle D,10f\rangle$	155.493						
$\langle E,6d\rangle$	155.572		155.34	155.05			
$\langle D\rangle$	Threshold						
$\langle E,7s\rangle$	155.628		155.37	155.17			
$\langle E,7d\rangle$	155.683		155.44	155.20			
$\langle E,8s\rangle$	155.721		155.47	155.26			
$\langle E,8d\rangle$	155.758		155.51	155.26			
$\langle E,9s\rangle$	155.770		155.53	155.34			
$\langle E,10s\rangle$	155.803			155.36			
$\langle E,9d\rangle$	155.809		155.56	155.32			
$\langle E,11s\rangle$	155.830						
$\langle E,10d\rangle$	155.843			155.36			
$\langle E\rangle$	Threshold						
$\langle F,3p\rangle$	157.228		157.15	156.97	156.97		
$\langle F,4p\rangle$	158.461		158.19	158.06	158.05		
$\langle F,5p\rangle$	158.969		158.63	158.51	158.50		
$\langle F,6p\rangle$	159.209		158.84	158.73	158.71		
$\langle F,7p\rangle$	159.344		158.97	158.86	158.84		
$\langle F,8p\rangle$	159.427		159.05	158.94			
$\langle F,9p\rangle$	159.482		159.10	158.99			
$\langle F\rangle$	Threshold						

$\langle C\rangle$ threshold the energy ordering of our states differ from BN in that we have the $\langle D,4f\rangle$ state below the $\langle D,4p\rangle$ state, whereas BN has the order reversed. We also have the $\langle E,4d\rangle$ state below the $\langle D,5p\rangle$ state in agreement with Vo Ky *et al.*, whereas BN has the opposite ordering. The energy ordering of the remaining states in Table VI are in complete agreement with BN. This ordering differs slightly from that of Vo Ky *et al.* in that they have the $\langle E,5d\rangle$ state below the $\langle D,7p\rangle$ state and they have the opposite ordering to ours for the $\langle D,9p\rangle$ and $\langle E,6s\rangle$ states.

In Table VII, we compare our quantum defects for the $\langle B,ns\,^2P^o\rangle$ and $\langle F,np\,^2P^o\rangle$ series with those of BN and Vo Ky *et al.* and with the experimental results of Diehl *et al.* [8].

We see that our quantum defects for the $\langle B,ns\,^2P^o\rangle$ series are in good agreement with those of BN and with experiment. However, our defects for the $\langle F,np\,^2P^o\rangle$ are not in agreement with either calculation or with experiment. This is due to the fact that our method yields a value for the $\langle F\rangle$ threshold that is too high.

C. The $^2S^e$ and $^2D^e$ series

Recently, the first photoexcitation measurements of triply excited even-parity states of lithium have been reported by Cubaynes *et al.* [6]. The lithium atoms in the ground $(1s)^2 2s\,^2S^e$ state were first excited to the $(1s)^2 2p\,^2P^o$ state by means of a cw dye laser. The dipole selection rules for laser excited atoms allow the population of even-parity hollow states that are not accessible from the ground state and which have angular momenta $^2S^e$, $^2P^e$, and $^2D^e$. The only previous experimental value for an even-parity hollow state was by Muller *et al.* [30], where a resonance in an electron-Li^+ collision experiment was attributed to a $2s(2p)^2\,^2D^e$ at 145 eV above the ground state.

TABLE VII. Comparison of quantum defects for B_s and F_p series with $^2P^o$ symmetry.

	$(2s2p)^3P\ ns\ ^2P^o$				$(2p)^2\,^1S^e\ np\ ^2p^o$			
n	This work	*BN*	Ky *et al.*	Expt.	This work	*BN*	Ky *et al.*	Expt.
3	0.71	0.68	0.66	0.65(2)	0.61	0.48	0.52	0.51(1)
4	0.79	0.67	0.68	0.62(3)	0.65	0.48	0.51	0.50(2)
5	0.75	0.70	0.69	0.68(3)	0.60	0.48	0.48	0.46(3)
6	0.75	0.71	0.63	0.73(5)	0.58	0.48	0.47	0.49(4)
7	0.69	0.71	0.60	0.77(6)	0.57	0.48	0.43	0.48(6)
8	0.73	0.72	0.65		0.56	0.48	0.39	
9	0.75	0.72	0.58		0.55	0.48	0.43	

TABLE VIII. Energies, n^*, and classification of $^2D^e$ states of Li. Note: See text for descriptions of configurations. State no. 1 is the first level for three series: $\langle B,2p\rangle$, $\langle D,2s\rangle$, and $\langle F,2s\rangle$.

No.	Config.	Energy	n^*	Description
1	$2s(2p)^2$	2.148041	1.34168	$70\%E_p$ $16\%B_p$ $6\%D_s$
2	$\langle A,3d\rangle$	1.961412	2.80425	$66\%A$ $8\%B_p$ $20\%F$
3	$\langle B,3p\rangle$	1.952783	2.46179	$80\%B_p$ $7\%A$
4	$\langle A,4d\rangle$	1.931865	3.83283	$71\%A$ $22\%F$
5	$\langle A,5d\rangle$	1.919264	4.82980	$72\%A$ $23\%B_p$
6	$\langle B,4p\rangle$	1.913228	3.41205	$58\%B_p$ $27\%A$ $8\%F$
7	$\langle A,6d\rangle$	1.912031	5.93375	$48\%A$ $61\%B_p$ $15\%F$
8	$\langle A,7d\rangle$	1.908423	6.87031	$72\%A$ $23\%F$
9	$\langle A,8d\rangle$	1.905898	7.87244	$72\%A$ $23\%F$
10	$\langle A,9d\rangle$	1.904171	8.87967	$73\%A$ $23\%F$
11	$\langle B,4f\rangle$	1.903320	3.89016	$95\%B_f$
12	$\langle A,10d\rangle$	1.902942	9.88987	$73\%A$ $23\%F$
13	$\langle A,11d\rangle$	1.902033	10.90653	$73\%A$ $23\%F$
$\langle A\rangle$	Threshold	1.897830		
18	$\langle B,5p\rangle$	1.895225	4.47707	$59\%B_p$ $27\%A$ $8\%F$
19	$\langle B,5f\rangle$	1.890856	4.92955	$94\%B_f$
21	$\langle B,6p\rangle$	1.887078	5.45580	$92\%B_p$
22	$\langle B,6f\rangle$	1.884446	5.94103	$95\%B_f$
23	$\langle B,7p\rangle$	1.882423	6.41685	$84\%B_p$ $8\%A$
25	$\langle B,7f\rangle$	1.880645	6.94546	$95\%B_f$
26	$\langle B,8p\rangle$	1.879299	7.44579	$93\%B_p$
27	$\langle B,8f\rangle$	1.878197	7.94722	$96\%B_f$
28	$\langle B,9p\rangle$	1.877320	8.42738	94^*B_p
29	$\langle B,9f\rangle$	1.876525	8.94799	$90\%B_f$
30	$\langle B,10p\rangle$	1.875922	9.41401	$95\%B_p$
31	$\langle B,10f\rangle$	1.875332	9.94822	$96\%B_f$
32	$\langle B,11p\rangle$	1.874900	10.40289	$95\%B_p$
33	$\langle B,11f\rangle$	1.874448	10.95334	$95\%B_f$
$\langle B\rangle$	Threshold	1.870280		
48	$\langle C,3d\rangle$	1.843620	2.92429	$65\%C$ $23\%B_f$ $6\%B_p$
50	$\langle E,3p\rangle$	1.834940	2.28587	$36\%E_p$ $16\%B_f$ $17\%D_d$ $8\%D_g$
52	$\langle C,4d\rangle$	1.816679	3.98227	$86\%C$ $4\%B_f$
53	$\langle D,3d\rangle$	1.812242	2.88816	$57\%D_d$ $13\%E_p$ $14\%D_s$
54	$\langle D,3s\rangle$	1.806939	3.02504	$29\%D_s$ $19\%C$ $11\%B_p$ $12\%E_p$
56	$\langle C,5d\rangle$	1.805107	5.00544	$40\%C$ 28^*D_s $12\%A$
57	$\langle C,6d\rangle$	1.799555	5.89163	$89\%C$ $3\%B_f$
58	$\langle C,7d\rangle$	1.795860	6.83282	$89\%C$ $3\%B_f$
59	$\langle C,8d\rangle$	1.793442	7.76539	$88\%C$ $4\%B_f$
60	$\langle C,9d\rangle$	1.791780	8.68423	$86\%C$ $3\%B_f$ $3\%B_p$
61	$\langle C,10d\rangle$	1.790644	9.53992	$66\%C$ $6\%D_d$ $6\%D_s$ $7\%B_p$
62	$\langle D,4d\rangle$	1.790275	3.62857	$29\%C$ $26\%D_d$ $24\%E_p$ $5\%D_s$
63	$\langle C,11d\rangle$	1.789612	10.58526	$84\%C$ $3\%D_d$ $2\%E_p$
$\langle C\rangle$	Threshold	1.785150		
70	$\langle E,4p\rangle$	1.780731	3.47183	$36\%E_p$ $29\%D_d$ $12\%B_p$ $7\%B_f$
71	$\langle D,4s\rangle$	1.778240	4.39032	$72\%D_s$ $7\%B_p$ $4\%E_p$ $5\%D_d$
72	$\langle E,4f\rangle$	1.776587	3.65942	$66\%E_f$ $22\%D_g$
74	$\langle D,5d\rangle$	1.772699	4.95082	$79\%D_d$ $8\%E_p$
75	$\langle D,5g\rangle$	1.770344	5.26400	$74\%D_g$ $14\%E_f$
76	$\langle D,5s\rangle$	1.769384	5.40992	$83\%D_s$ $4\%E_p$
77	$\langle D,6d\rangle$	1.766537	5.92622	$70\%D_d$ $17\%E_p$
79	$\langle D,6g\rangle$	1.764988	6.27745	$84\%D_g$ $4\%E_f$
80	$\langle D,6s\rangle$	1.764470	6.40966	$52\%D_s$ $22\%E_p$ $13\%D_d$
81	$\langle E,5p\rangle$	1.763497	4.54100	$38\%D_s$ $24\%D_d$ $28\%E_p$

TABLE VIII. (*Continued*.)

No.	Config.	Energy	n^*	Description
82	$\langle D,7d\rangle$	1.761733	7.28060	$73\%D_d$ $10\%E_p$ $3\%D_s$
83	$\langle D,7g\rangle$	1.761630	7.32040	$76\%D_g$ $12\%E_f$
84	$\langle D,7s\rangle$	1.760699	7.71541	$82\%D_s$ $3\%E_p$ $3\%D_d$
85	$\langle E,5f\rangle$	1.760110	4.89582	$55\%E_f$ $32\%D_g$
86	$\langle D,8d\rangle$	1.759388	8.39892	$84\%D_d$ $4\%E_p$
87	$\langle D,8g\rangle$	1.758834	8.74744	$75\%D_g$ $13\%E_f$
88	$\langle D,8s\rangle$	1.758599	8.90961	$86\%D_s$ $2\%E_p$
89	$\langle D,9d\rangle$	1.757711	9.61252	$84\%D_d$ $4\%E_p$
90	$\langle D,9g\rangle$	1.757356	9.95570	$85\%D_g$ $3\%E_f$
91	$\langle D,9s\rangle$	1.757124	10.18028	$86\%D_s$ $3\%E_p$
92	$\langle D,10d\rangle$	1.756520	10.88467	$80\%D_d$ $7\%E_p$
98	$\langle E,6p\rangle$	1.755045	5.62635	$40\%D_s$ $33\%D_d$ $15\%E_p$
104	$\langle E,6f\rangle$	1.752960	6.03907	$58\%E_f$ $29\%D_g$
$\langle D\rangle$	Threshold	1.752300		
109	$\langle E,7p\rangle$	1.750249	6.74216	$50\%E_p$ $20\%D_s$ $18\%D_d$
112	$\langle E,7f\rangle$	1.748690	7.27761	$57\%E_f$ $30\%D_g$
113	$\langle E,8p\rangle$	1.747489	7.79002	$53\%E_p$ $32\%D_s$ $3\%D_d$
115	$\langle E,8f\rangle$	1.746438	8.34035	$81\%E_f$ $6\%D_g$
116	$\langle E,9p\rangle$	1.745363	9.04395	$72\%E_p$ $13\%D_d$
117	$\langle E,9f\rangle$	1.745006	9.31991	$41\%E_f$ $47\%D_g$
120	$\langle E,10p\rangle$	1.743660	10.64818	$65\%E_p$ $17\%D_d$ $2\%D_s$ $3\%C$
121	$\langle E,10f\rangle$	1.743344	11.05144	$83\%E_f$ $3\%D_g$
$\langle E\rangle$	Threshold	1.739250		
150	$\langle F,3d\rangle$	1.656244	3.05440	$40\%E_f$ $11\%A$ $31\%F$
152	$\langle F,4d\rangle$	1.636257	3.85719	$50\%F$ $18\%A$ $11\%E_f$
153	$\langle F,5d\rangle$	1.624604	4.77227	$58\%F$ $20\%A$ $3\%E_f$
154	$\langle F,6d\rangle$	1.617715	5.76102	$60\%F$ $21\%A$
155	$\langle F,7d\rangle$	1.613588	6.76093	$60\%F$ $21\%A$
156	$\langle F,8d\rangle$	1.610943	7.76468	$60\%F$ $21\%A$
157	$\langle F,9d\rangle$	1.609149	8.77109	$60\%F$ $21\%A$
158	$\langle F,10d\rangle$	1.607878	9.77997	$61\%F$ $21\%A$
159	$\langle F,11d\rangle$	1.606942	10.79344	$61\%F$ $21\%A$
$\langle F\rangle$	Threshold	1.602650	⋯	⋯

In the $^2D^e$ case we have 10 series converging on the doubly excited states of Li^+. They are labeled in the following manner:

$$\langle A\rangle \quad (2s)^2\,{}^1S^e\,nd, \qquad \langle B_p\rangle \quad (2s2p)\,{}^3P^o\,np, \qquad \langle B_f\rangle \quad (2s2p)\,{}^3P^o\,nf, \qquad \langle C\rangle \quad (2p)^2\,{}^3P^e\,nd,$$
$$\langle D_s\rangle \quad (2p)^2\,{}^1D^e\,ns, \qquad \langle D_d\rangle \quad (2p)^2\,{}^1D^e\,nd, \qquad \langle D_g\rangle \quad (2p)^2\,{}^1D^e\,ng, \qquad \langle E_p\rangle \quad (2s2p)\,{}^1P^o\,np$$
$$\langle E_f\rangle \quad (2s2p)\,{}^1P^o\,nf, \qquad \langle F\rangle \quad (2p)^2\,{}^1S^e\,nd.$$

We note that the state with the lowest energy, i.e., $E_n=-2.148\,041$, is common to series $\langle B_p\rangle$, $\langle D_s\rangle$, and $\langle E_p\rangle$. That is to say, the state can be described as $(2s2p)^3P^o\,2p$, or $(2p)^2\,{}^1D^e\,2s$, or $(2s2p)^1P^o\,2p$.

The phenomenon observed in Sec. III B as related to Eq. (11) also occurs for the $\langle A,nd\rangle$ and $\langle F,nd\rangle$ series with $^2D^e$ symmetry. As can be seen in Table VIII, the higher members of the $\langle A,nd\rangle$ series are described with remarkable consistency as being 73%*A* and 23%*F*, while the higher members of the $\langle F,nd\rangle$ series are described by 21%*A* and 61%*F*. These are (to less than 0.5%) the same numbers as was seen previously for the $^2P^o$ symmetry. What is equally remarkable is that the exact same numbers appear in the equivalent series for $^2S^e$ symmetry. These mixtures are displayed in Table IX.

The $^2S^e$ series is included for completeness as there are some theoretical results with which we can compare. Again we note that the state with the lowest energy, i.e., $E_n=-2.082\,745$, is common to three series, the equivalent de-

TABLE IX. Energies, n^*, and classification of $^2S^e$ states of Li. Note: State no. 1 is the first member of three series: $\langle B,2p\rangle$, $\langle E,2p\rangle$, and $\langle F,2s\rangle$.

No.	Config.	Energy	n^*	Description
1	$2s(2p)^2$	2.082745	1.53406	60%E 21%B 9%F6%A
2	$\langle A,3s\rangle$	2.004837	2.16162	67%A 18%F 6%E 6%B
3	$\langle A,4s\rangle$	1.950938	3.06836	63%A 20%F 13%B
4	$\langle B,3p\rangle$	1.941499	2.64963	73%B 13%A 5%E
5	$\langle A,5s\rangle$	1.926483	4.17736	71%A 22%F
6	$\langle A,6s\rangle$	1.916524	5.17165	71%A 22%F
7	$\langle A,7s\rangle$	1.911052	6.14937	69%A 22%F
8	$\langle B,4p\rangle$	1.908422	3.62063	64%B 23%A 7%F
9	$\langle A,8s\rangle$	1.907219	7.29754	58%A 19%B 18%F
10	$\langle A,9s\rangle$	1.905205	8.23380	71%A 26%F
11	$\langle A,10s\rangle$	1.903699	9.23026	73%A 23%F
12	$\langle A,11s\rangle$	1.902602	10.23651	73%A 23%F
$\langle A\rangle$	Threshold	1.897830		
18	$\langle B,5p\rangle$	1.893236	4.66697	68%B 20%A 6%F
20	$\langle B,6p\rangle$	1.885879	5.66161	90%B 3%A
21	$\langle B,7p\rangle$	1.881593	6.64803	95%B
22	$\langle B,8p\rangle$	1.878837	7.64406	95%B
23	$\langle B,9p\rangle$	1.876978	8.63978	95%B
24	$\langle B,10p\rangle$	1.875668	9.63310	95%B
25	$\langle B,11p\rangle$	1.874714	10.61891	94%B
26	$\langle B,12p\rangle$	1.874007	11.58202	63%B 25%A
$\langle B\rangle$	Threshold	1.870280		
33	$\langle E,3p\rangle$	1.846667	2.15749	30%E 28%A 15%B 11%F
36	$\langle D,3d\rangle$	1.806143	3.04733	69%D 13%E 4%B
37	$\langle E,4p\rangle$	1.792245	3.07163	60%E 17%D 10%B
$\langle C\rangle$	Threshold	1.785150		
38	$\langle D,4d\rangle$	1.781501	4.13793	71%D 11%B 6%E
39	$\langle D,5d\rangle$	1.771887	5.05248	74%D 13%B
40	$\langle E,5p\rangle$	1.770730	3.98535	55%E 24%B 9%D
41	$\langle D,6d\rangle$	1.765940	6.05450	76%D 7%E 4%B
42	$\langle D,7d\rangle$	1.762628	6.95793	55%D 24%E 7%B
43	$\langle E,6p\rangle$	1.760917	4.80382	55%D 28%E 3%B
44	$\langle D,8d\rangle$	1.759141	8.54947	10%E 78%D
45	$\langle D,9d\rangle$	1.757609	9.70417	81%D 6%E
46	$\langle D,10d\rangle$	1.756471	10.94915	80%D 7%E
49	$\langle E,7p\rangle$	1.754309	5.76221	22%E 65%D 1%B
$\langle D\rangle$	Threshold	1.752300		
52	$\langle E,8p\rangle$	1.750266	6.73711	55%E 31%D
54	$\langle E,9p\rangle$	1.747106	7.97769	70%E 17%D
55	$\langle E,10p\rangle$	1.745415	9.00576	74%E 13%D
56	$\langle E,11p\rangle$	1.744219	10.03097	65%E 23%D
57	$\langle E,12p\rangle$	1.743368	11.01911	65%E 23%D
$\langle E\rangle$	Threshold	1.739250		
70	$\langle F,3s\rangle$	1.655855	3.06554	52%F 20%A 10%D
72	$\langle F,4s\rangle$	1.629691	4.30003	55%F 20%A 5%D
73	$\langle F,5s\rangle$	1.620510	5.29106	60%F 21%A
74	$\langle F,6s\rangle$	1.615289	6.28978	60%F 22%A
75	$\langle F,7s\rangle$	1.613055	6.93217	60%F 22%A
76	$\langle F,8s\rangle$	1.612000	7.31280	59%F 22%A
77	$\langle F,9s\rangle$	1.609889	8.31085	61%F 21%A
78	$\langle F,10s\rangle$	1.608409	9.31800	61%F 21%A
79	$\langle F,11s\rangle$	1.607337	10.32833	61%F 21%A
$\langle F\rangle$	Threshold	1.602650		

TABLE X. Comparison of some even-parity triply excited $^2L^e$ $(L=S,P,D)$ states for Li.

State	This work	Chung	*BN*	Zhou *et al.*	Experiment
$2s(2p)^2\ ^2D^e$	144.844	144.762	144.826	144.664	144.77
$2s(2p)^2\ ^2S^e$	146.621	146.480	146.612	146.534	
$2s(2p)^2\ ^2P^e$	147.037	146.923	147.012	146.910	146.93
$\langle A,3s\ ^2S^e\rangle$	148.741	148.794	148.822	148.632	
$\langle B,3p\ ^2P^e\rangle$	149.644	149.713	149.742	149.548	
$\langle A,3d\ ^2D^e\rangle$	149.923	149.999	149.982	149.826	
$\langle B,3p\ ^2D^e\rangle$	150.158	150.212	150.233	150.045	
$\langle A,4s\ ^2S^e\rangle$	150.208	150.264	150.181	150.064	
$\langle B,3p\ ^2S^e\rangle$	150.465	150.499	150.520	150.337	
$\langle A,4d\ ^2D^e\rangle$	150.727		150.651	150.484	
$\langle C,3s\ ^2P^e\rangle$	152.185	152.129	152.253	152.055	
$\langle C,3d\ ^2P^e\rangle$	152.978	153.003	153.050	152.860	
$\langle C,3d\ ^2D^e\rangle$	153.128	153.174	153.245	153.032	
$\langle C,4s\ ^2P^e\rangle$	153.555	153.458	153.540	153.365	
$\langle D,3d\ ^2P^e\rangle$	154.114	154.393	154.093	153.834	
$\langle D,3d\ ^2S^e\rangle$	154.148	154.313	154.093	153.950	
$\langle D,3s\ ^2D^e\rangle$	154.126	153.184	152.543	152.364	
$\langle D,4d\ ^2S^e\rangle$	154.819	155.064	154.625	154.483	
$\langle F,3s\ ^2S^e\rangle$	158.238	154.689	156.838	156.675	

scriptions being $(2s2p)^3P^o\,2p$ or $(2s2p)^1P^o\,2p$ or $(2p)^2\,^1S^e\,2s$. The results are presented in Table IX.

In Table X we compare our results for the even-parity states with available experimental [6] and theoretical results. The order in which the levels are given is based on our calculations.

The energies in Table X are given in eV above the ground state of lithium. In comparing our results with the saddle-point method of Chung and co-workers, where his results for the higher even-parity triply excited states were not quoted in eV [25], we have used his ground-state energy for lithium $-7.478\,678$ and 1 a.u. $=27.209\,27$ eV In the fourth column we compare with the *R*-matrix results of Zhou *et al.* [31], who have quoted energies relative to the first excited $(1s)^2\,2p$ state of lithium and where we have assumed that $E[(1s)^2\,2p]-E[(1s)^2\,2s]=1.848$ eV. We see that the results agree very well—the exceptions being $\langle D,3s\ ^2D^e\rangle$ and the $\langle F,3s\ ^2S^e\rangle$ state. Our $\langle D,3s\ ^2D^e\rangle$ state at 154.126 eV is the lowest member of this series that we could identify and should probably be labeled $\langle D,4s\ ^2D^e\rangle$, which would agree well with the $\langle D,4s\ ^2D^e\rangle$ at 154.050 of BN. This is the only mismatch which we have found between their results and ours. The energy of our $\langle F,3s\ ^2S^e\rangle$ state at 158.238 eV is too high in comparison with the other calculations as our two-electron $\langle F\rangle$ threshold obtained by the TDM method too high. It would appear that the Chung [25] calculation for this state is too low.

IV. CONCLUSION

The theoretical procedure described in this paper yields consistent sequences of energy levels and quantum defects for each Rydberg-like series. We see that our energy levels are too high by about 0.2 eV when compared to the more accurate calculations of Chung. The advantage of the method is that it provides us with whole series all at once and enables us to unambiguously classify the levels using both configuration mixings and quantum defect. Further experimental data and calculations are required to resolve conflicts in our present knowledge of triply excited states.

[1] L. M. Kiernan, E. T. Kennedy, J. P. Mosnier, J. T. Costello, and B. F. Sonntag, Phys. Rev. Lett. **72**, 2359 (1994).

[2] L. M. Kiernan, M. K. Lee, B. F. Sonntag, P. Sladeczek, P. Zimmerman, E. T. Kennedy, J. P. Mosnoir, and J. T. Costello, J. Phys. B **28**, L161 (1995).

[3] Y. Azuma, S. Hasegawa, F. Koilke, G. Kutluk, T. Nagata, E. Shigemasa, A. Yagashita, and I. Sellin, Phys. Rev. Lett. **74**, 3768 (1995).

[4] L. Journel, D. Cubaynes, J. M. Bizau, S. Al Moussalami, B. Rouvellou, F. Wuillemier, L. Vo Ky, P. Faucher, and A. Hibbert, Phys. Rev. Lett. **76**, 30 (1996).

[5] S. Diehl, D. Cubaynes, J. M. Bizau, L. Journel, B. Rouvellou, S. Al Moussalami, F. Wuillemier, E. T. Kennedy, N. Barrah, C. Blanchard, T. J. Morgan, J. Bozek, A. S. Schlacter, L. Vo Ky, P. Faucher, and A. Hibbert, Phys. Rev. Lett. **76**, 3915 (1996).

[6] D. Cubaynes, S. Diehl, L. Journel, B. Rouvellou, J. M. Bizau, S. Al Moussalami, F. Wuillemier, N. Barrah, L. Vo Ky, P. Faucher, A. Hibbert, C. Blankard, E. Kennedy, J. T. Morgan, J. Bozek, and A. S. Schlacter, Phys. Rev. Lett. **77**, 2194

(1996).
[7] L. Journel, D. Cubaynes, J. M. Bizau, S. Al Moussalami, B. Rouvellou, F. Wuillemier, L. Vo Ky, P. Faucher, and A. Hibbert, Phys. Rev. Lett. **76**, 30 (1996).
[8] E. T. Kennedy, J. T. Costello, and J. P. Mosnier, J. Electron. Spectrosc. Relat. Phenom. **79**, 283 (1996).
[9] S. Diehl, D. Cubaynes, E. T. Kennedy, F. Wuillemier, J. M. Bizau, L. Journel, L. Vo Ky, P. Faucher, A. Hibbert, C. Blankard, N. Barrah, T. J. Morgan, J. Bozek, and A. S. Schlacter, J. Phys. B **30**, L1 (1997).
[10] S. Diehl, D. Cubaynes, K. T. Chung, F. Wuillemier, E. T. Kennedy, J. M. Bizau, L. Journel, C. Blanchard, L. Vo Ky, P. Faucher, A. Hibbert, N. Barrah, T. J. Morgan, J. Bozek, and A. S. Schlacter, Phys. Rev. A **56**, R1074 (1997).
[11] S. Diehl, D. Cubaynes, J. M. Bizau, F. Wuillemier, E. T. Kennedy, L. Vo Ky, C. Blanchard, T. J. Morgan, N. Barrah, J. Bozek, A. S. Schlacter, A. Hibbert, and P. Faucher (unpublished); see also S. Diehl, D. Cubaynes, F. Wuillemier, E. T. Kennedy, C. Blanchard, K. T. Chung, L. Vo Ky, J. M. Bizau, T. J. Morgan, N. Barrah, J. Bozek, A. S. Schlacter, A. Hibbert, and P. Faucher (unpublished).
[12] S. Diehl, D. Cubaynes, F. Wuillemier, J. M. Bizau, L. Journel, E. T. Kennedy, C. Blanchard, L. Vo Ky, P. Faucher, A. Hibbert, N. Barrah, T. J. Morgan, J. Bozek, and A. S. Schlacter, Phys. Rev. Lett. **79**, 1241 (1997).
[13] Kwong T. Chung and Bing-Cong Gou, Phys. Rev. A **52**, 3669 (1995).
[14] Kwong T. Chung and Bing-Cong Gou, Phys. Rev. A **53**, 2189 (1996).
[15] U. Fano, Phys. Rev. **124**, 1866 (1961).
[16] D. R. Herrick and Oktay Sinanoglu, Phys. Rev. A **11**, 97 (1975).
[17] M. J. Conneely and L. Lipsky, J. Phys. B **11**, 4135 (1978).
[18] R. Bruch, G. Paul, J. Andra, and L. Lipsky, Phys. Rev. A **12**, 1808 (1975).
[19] M. Rodbro, R. Bruch, and P. Bisgaard, J. Phys. B **12**, 2412 (1979).
[20] M. Ahmed and L. Lipsky, Phys. Rev. A **12**, 1176 (1976).
[21] M. J. Conneely, L. Lipsky, and A. Russek, Phys. Rev. A **46**, 4012 (1992).
[22] L. Lipsky, R. Anania, and M. J. Conneely, At. Data Nucl. Data Tables **20**, 127 (1977).
[23] Keith Berrington and Shinobu Nakazaki, J. Phys. B **31**, 313 (1998).
[24] L. Vo Ky, P. Faucher, H. L. Zhou, A. Hibbert, Y.-Z. Qu, J.-M. Li, and F. Bely-Dubau, Phys. Rev. A **58**, 3688 (1978).
[25] Ying Zhang and Kwong T. Chung, Phys. Rev. A **58**, 1098 (1998).
[26] D. K. McKenzie and G. W. F. Drake, Phys. Rev. A **44**, R6973 (1991).
[27] K. T. Chung as quoted in Ref. [9].
[28] J. P. Buchet, M. C. Buchet-Poulizac, and H. G. Berry, Phys. Rev. A **7**, 922 (1973).
[29] T. Andersen, S. M. Bentzen, and O. Poulsen, Phys. Scr. **22**, 119 (1980).
[30] A. Muller, G. Hoffmann, B. Weissbecker, M. Stenke, K. Tinschert, M. Wagner, and E. Salzborn, Phys. Rev. Lett. **63**, 758 (1989).
[31] H. L. Zhou, S. T. Manson, L. Vo Ky, P. Faucher, F. Bely-Dubau, A. Hibbert, S. Diehl, D. Cubaynes, J.-M. Bizau, L. Journel, and F. J. Wuilleumier, Phys. Rev. A **59**, 462 (1999).